Original Article

Development and validation of the nomogram based on ultrasound, thyroid stimulating hormone, and inflammatory marker in papillary thyroid carcinoma: a case-control study

Zhong-Wei Tang[#^], Xin-Xi Li[#], Jun Luo

Department of Vascular Thyroid Surgery, The First Affiliated Hospital of Xinjiang Medical University, Urumqi, China

Contributions: (I) Conception and design: ZW Tang, J Luo; (II) Administrative support: J Luo; (III) Provision of study materials or patients: XX Li; (IV) Collection and assembly of data: XX Li; (V) Data analysis and interpretation: ZW Tang, XX Li; (VI) Manuscript writing: All authors; (VII) Final approval of manuscript: All authors.

[#]These authors contributed equally to this work.

Correspondence to: Jun Luo. Department of Vascular Thyroid Surgery, The First Affiliated Hospital of Xinjiang Medical University, Urumqi 830000, China. Email: xmuluo@163.com.

Background: The increase in the number of thyroid cancer cases in recent years has increased not only the medical burden but also the potential for overtreatment. Therefore, it is crucial to distinguish papillary thyroid cancer from benign thyroid nodules before surgery when treating thyroid nodules.

Methods: The patients were divided into two groups: 117 patients made up the validation cohort and 414 patients made up the primary cohort. As a result of the primary cohort, a preoperative prediction model was developed, which was then validated externally in the validation cohort. Preoperative thyrotropin (thyroid stimulating hormone, TSH), systemic immune-inflammation index (SII), lymphocyte-to-monocyte ratio (LMR), and ultrasonographic features were recorded in both groups.

Results: As predictors for the model, the preoperative blood levels of TSH, SII, LMR, echogenicity, margin, calcification, composition, taller-than-wide, and age were chosen. This was the regression equation: Y = −0.070 × (age) + 1.511 × (echogenicity) + 1.664 × (margin) + 1.003 × (calcification) + 0.939 × (composition) + 2.964 × (tall than wide) + 0.305 × (TSH) + 0.558 × (SII) − 1.271 × (LMR) + 0.327. Papillary thyroid carcinoma (PTC) was predicted positively with values of Y ≥0.808. The prediction model's accuracy, sensitivity, and specificity were 88.2%, 85.1%, and 94.9%, respectively. The area under the receiver operating characteristic (ROC) curve was 0.961. The model's external validation produced satisfactory results with accuracy, sensitivity, and specificity of 85.5%, 90.9%, and 75.5%, respectively.

Conclusions: Using the preoperative TSH, SII, LMR, and ultrasonographic characteristics, a straightforward and accurate preoperative prediction model for PTC has been developed and validated. The preoperative assessment of PTC in clinical application is enhanced by this approach.

Keywords: Papillary thyroid carcinoma (PTC); diagnosis model; thyroid stimulating hormone (TSH); systemic immune-inflammation index (SII); lymphocyte-to-monocyte ratio (LMR)

Submitted Oct 25, 2022. Accepted for publication Feb 19, 2023. Published online Mar 17, 2023.
doi: 10.21037/tcr-22-2478
View this article at: https://dx.doi.org/10.21037/tcr-22-2478

^ ORCID: 0000-0003-1602-0068.

Introduction

Thyroid carcinoma (TC) is the most common malignant tumor of the endocrine system and is classified into papillary, follicular, medullary, and undifferentiated carcinomas. It is estimated that 70–75% of thyroid malignancies are papillary carcinomas, while 15–20% are follicular carcinomas (1). In the previous 20 years, their incidence has risen by 21%, with a higher incidence of low-risk papillary thyroid microcarcinomas (PTMCs) (2,3). However, there has been no significant change in thyroid cancer-related mortality, mainly due to overdiagnosis and overtreatment of thyroid cancer as a result of improved and widely available ultrasound technology (4). The treatment of papillary thyroid carcinoma (PTC) mainly includes surgical resection and radioactive iodine therapy, and the 5-year overall survival (OS) rate is 98.2% (5). Although the prognosis for PTC is promising after surgery, overtreatment can place an unnecessary burden of disease on patients. One of the costliest malignancies to treat in the US is PTC. Treatment expenses are projected to reach around $1.6 billion in 2013 and to increase by 2030 (6).

Currently, the gold standard for the differential diagnosis of benign and malignant thyroid tumors is pathological diagnosis. However, high-frequency ultrasound, which allows real-time dynamic observation of the lesion and surrounding structures and has the advantages of being noninvasive, radiation-free, and reproducible (7), is the test of choice for identifying benign and malignant thyroid nodules. In PTC, several ultrasonography characteristics, such as hypoechogenicity, irregular margins, taller-than-wide, and microcalcifications, are linked to malignancy (8,9).

PTC and other neoplastic disorders are well known to be influenced by cancer-associated inflammation (10). The immune and inflammatory response is a double-edged sword in tumorigenesis, development, and prognosis, which not only destroys tumor cells but also promotes tumor growth by establishing a microenvironment conducive to tumor growth (11). Since routine blood tests could, at least in part, reflect inflammatory responses, the role of hematological markers as prognostic indicators or cancer predictions was the main study topic. Systemic immune-inflammation index (SII) and the lymphocyte-to-monocyte ratio (LMR) have been well-studied in many malignancies (12,13). However, there is little research on the relationships between these inflammatory indicators and PTC. Thyrotropin (thyroid stimulating hormone, TSH) may influence the onset or progression of thyroid cancer generated from follicular cells (14). A sensitive surrogate for thyroid function, serum TSH also controls thyroid cell differentiation (15). Patients with thyroid nodules who have low TSH levels are less likely to have nodules that are malignant. Since patients with papillary thyroid cancer usually have a good prognosis, the increase in the number of cases in recent years has not only increased the medical burden but also the possibility of overtreatment at the same time, so a precise preoperative diagnosis is crucial.

Therefore, this study developed and validated an accessible nomogram that combines ultrasound features, TSH, and inflammatory markers to identify benign and malignant thyroid nodules and compared it with the diagnostic efficacy of Thyroid Imaging Reporting and Data System (TI-RADS) classification (16), to further improve diagnostic efficacy and guide clinical interventions against tumors. We present the following article in accordance with the TRIPOD reporting checklist (available at https://tcr.amegroups.com/article/view/10.21037/tcr-22-2478/rc).

Highlight box

Key findings

- We found that the model consisting of inflammatory markers combined with TSH and ultrasound signs had better diagnostic efficacy.

What is known and what is new?

- Ultrasound is the primary screening modality for thyroid cancer because of its cost-effectiveness and convenience, but there is a problem of overdiagnosis and overtreatment. There is a need for a more effective diagnostic method to reduce the medical burden and overtreatment of patients.
- In this study, we constructed a diagnostic model combining inflammatory markers with TSH and ultrasound signs and found its diagnostic efficacy to be superior to the TI-RADS classification.

What is the implication, and what should change now?

- The model we have constructed may help in the diagnosis of papillary thyroid cancer, but still needs to be validated with large data.

Methods

Study population

The First Affiliated Hospital of Xinjiang Medical University's ethical committee accepted this retrospective case-control research (No. K202206-02). The sample size is calculated based on EPV (Events per variable). A group of thyroid illness patients were hospitalized at the Vascular Thyroid Surgery Department at Xinjiang

Medical University's First Affiliated Hospital. The patients were divided into two groups: the primary cohort, which included data from patients admitted between January 2020 and July 2020 and totally 414 patients with 500 nodes; and the validation cohort, which included data from patients admitted between December 2021 and March 2022 and totally 117 patients with 152 nodes. All patients gave their informed permission. Two experienced pathologists examined the postoperative histopathology. The study was conducted in accordance with the Declaration of Helsinki (as revised in 2013). Individual consent for this retrospective analysis was waived.

Ultrasound examination

The sonographic exams were carried out using a LOGIQ E9 US scanner (GE Healthcare, Chalfont St. Giles, UK). One radiologist with at least ten years of expertise conducted the standard ultrasound. All ultrasound images were reviewed blindly by two radiologists with 10 years of thyroid experience. When discrepancies arose, an agreement was reached after discussion. Study subjects were positioned supine with their necks extended to completely expose the thyroid area. Each nodule's echogenicity, margin, shape, echotexture, calcification, composition, and tall-than-wide were all noted on the ultrasound.

TSH, SII, and LMR detection

Immunochemiluminescent techniques were used to assess the serum TSH content in each patient before surgery. 0.27 to 4.2 mIU/L was designated as the usual range. From a preoperative routine blood test, complete platelet, neutrophil, lymphocyte, and monocyte counts were obtained. Multiplying the total neutrophil count by the total platelet count and dividing it by the total lymphocyte count yields the SII value. By dividing the total lymphocyte count by the total monocyte count, the value of LMR was determined.

Inclusion and exclusion criteria

This study included the following criteria for inclusion: (I) Thyroidectomy patients; (II) patients are assessed by regular postoperative histopathology and intraoperative frozen sections; (III) cases completed preoperative thyroid conventional ultrasound examination and serological examination.

Patients were excluded if: (I) circumstances when ultrasonography and preoperative serum inflammatory marker values were unavailable; (II) ultrasonography imaging has shown instances of widespread thyroid lesions without visible nodules; (III) patients who have previously undergone thyroid cancer surgery; (IV) cases of follicular neoplasms with unclear malignant potential or other types of thyroid malignancy.

Statistical analysis

Statistical analysis was conducted with the R software (version 4.0.1; http://www.Rproject.org). The median and interquartile range were used to represent continuous variables that are not normally distributed, and the Mann-Whitney U test was used to compare groups. Comparing categorical data was done using the Chi-square test or Fisher exact test. The linear relationship between the continuous variable and the dependent variable is judged by the restriction cubic spline, and the continuous variable with nonlinear correlation is converted to categorical variables with the median as the boundary. All variables were included in the multivariate logistic regression analysis, then the backward selection method was used to screen variables and build a prediction model. Univariate analyses were computed with the "tableone" package. The "rms" software was used to perform multivariate binary logistic regression, nomogram, calibration plots, internal validation, and decision curve analysis. The "rms" package was used for external validation.

Development of an individualized prediction model

Patients in the primary cohort were divided into the PTC and non-PTC groups based on postoperative pathologic examination data; PTC was the only thyroid disease not included in the non-PTC group. The following index was used to begin the multivariate binary logistic regression analysis: age, gender, TSH, SII, LMR, echogenicity, margin, shape, echotexture, calcification status, composition, and tall than wide. Multivariable were chosen and employed to construct a diagnosis model for PTC utilizing the data from the primary cohort based on backward selection method and clinical relevance. To statistically forecast a person's likelihood of PTC, we created a nomogram.

Nomogram performance and validation in the primary cohort

Brier score and calibration curves were used to evaluate the calibration of the nomograms. The area under curve (AUC)

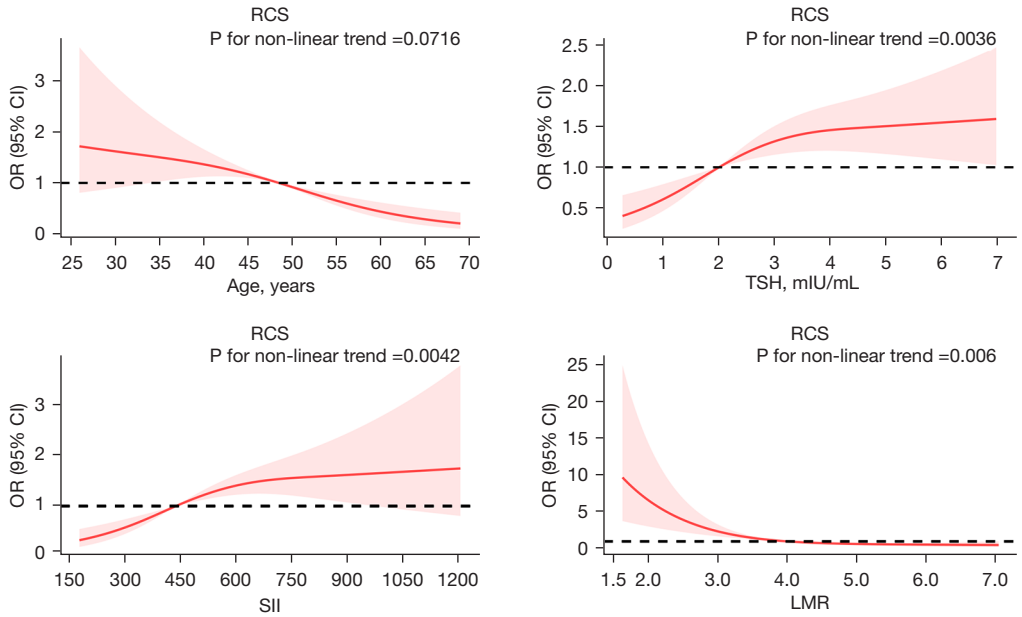

Figure 1 RCS. Association between continuity variables (age, TSH, SII, and LMR) and papillary thyroid carcinoma. OR, odds ratio; RCS, restricted cubic splines; TSH, thyrotropin; SII, systemic immune-inflammation index; LMR, lymphocyte-to-monocyte ratio.

was assessed using receiver operating characteristic (ROC) curve analysis to quantify the diagnostic model for PTC's performance in terms of discrimination and to compare it with the diagnostic performance of TI-RADS classification. Based on the primary cohort, the diagnostic model was internally validated by using the enhanced bootstrap method, and the concordance index (C-index) and brier scores were calculated.

In the validation cohort, the nomogram's effectiveness was evaluated. To compute the total points for each patient, the logistic regression algorithm created in the primary cohort was applied to all patients in the validation cohort. The entire number of points was then factored into binary logistic regression for this cohort. Finally, the brier score and AUC were obtained.

Clinical use

By calculating the net benefit under various threshold probabilities using decision curve analysis, the clinical utility of this nomogram was examined.

Results

Patients' characteristics

Five hundred participants made up the primary cohort (343 in the PTC group and 157 in the non-PTC group, respectively), while 152 made up the validation cohort (99 and 53 in the PTC and non-PTC groups, respectively). In *Figure 1*, we used restricted cubic splines to judge the linear relationship between the continuous variable and the dependent variable. TSH, SII, and LMR (P for non-linearity <0.05) were converted to categorical variables using their median as the cut-off. *Table 1* lists the patient characteristics for the primary and validation groups. Age, TSH, SII, LMR, echogenicity, margin, shape, echotexture, calcification, composition, tall-than-wide, and TI-RDAS classification were all significantly different in the primary cohort between PTC and non-PTC (P<0.05), and the majority of these differences were then validated in the validation cohort.

Development of an individualized prediction model

In the primary cohort, a logistic regression analysis revealed numerous independent predictors (*Table 2*), which were then utilized to create the nomogram (*Figure 2*). On multivariate logistic regression analysis, age [odds ratio (OR): 0.932, 95% confidence interval (CI): 0.901–0.963], echogenicity (OR: 4.533, 95% CI: 1.711–12.542), margin (OR: 5.281, 95% CI: 2.540–11.197), calcification (OR: 2.429, 95% CI: 1.286–5.928), tall than wide (OR: 19.371, 95% CI: 9.239–44.056),

Table 1 Characteristics of patients in the primary cohort and validation cohort

Characteristics	Primary cohort			Validation cohort		
	Non-PTC (n=157)	PTC (n=343)	P	Non-PTC (n=53)	PTC (n=99)	P
Age (years), median [IQR]	53.00 [47.00, 59.00]	46.00 [37.00, 54.00]	<0.001	48.00 [35.00, 56.00]	47.00 [36.00, 55.00]	0.675
Gender, n (%)						
Male	41 (26.1)	76 (22.2)	0.363	8 (15.1)	18 (18.2)	0.822
Female	116 (73.9)	267 (77.8)		45 (84.9)	81 (81.8)	
Echogenicity, n (%)						
hyperechoic or isoechoic	105 (66.9)	20 (5.8)	<0.001	39 (73.6)	9 (9.1)	<0.001
hypoechoic or markedly	52 (33.1)	323 (94.2)		14 (26.4)	90 (90.9)	
Margin, n (%)						
Clear	130 (82.8)	63 (18.4)	<0.001	47 (88.7)	27 (27.3)	<0.001
Unclear	27 (17.2)	280 (81.6)		6 (11.3)	72 (72.7)	
Shape, n (%)						
Regular	124 (79.0)	57 (16.6)	<0.001	46 (86.8)	18 (18.2)	<0.001
Irregular	33 (21.0)	286 (83.4)		7 (13.2)	81 (81.8)	
Echotexture, n (%)						
Homogeneous	59 (37.6)	7 (2.0)	<0.001	20 (37.7)	4 (4.0)	<0.001
Heterogeneous	98 (62.4)	336 (98.0)		33 (62.3)	95 (96.0)	
Calcification, n (%)						
No	134 (85.4)	164 (47.8)	<0.001	48 (90.6)	34 (34.3)	<0.001
Yes	23 (14.6)	179 (52.2)		5 (9.4)	65 (65.7)	
Composition, n (%)						
Cystic or spongiform	82 (52.2)	16 (4.7)	<0.001	31 (58.5)	6 (6.1)	<0.001
Solid	75 (47.8)	327 (95.3)		22 (41.5)	93 (93.9)	
Tall than wide, n (%)						
<1	140 (89.2)	75 (21.9)	<0.001	43 (81.1)	38 (38.4)	<0.001
≥1	17 (10.8)	268 (78.1)		10 (18.9)	61 (61.6)	
TSH (mIU/mL), n (%)						
<2	89 (56.7)	150 (43.7)	0.009	34 (64.2)	52 (52.5)	0.175
≥2	68 (43.3)	193 (56.3)		19 (35.8)	47 (47.5)	
SII, n (%)						
<439	101 (64.3)	148 (43.1)	<0.001	27 (50.9)	54 (54.5)	0.734
≥439	56 (35.7)	195 (56.9)		26 (49.1)	45 (45.5)	
LMR, n (%)						
<4	45 (28.7)	194 (56.6)	<0.001	19 (35.8)	27 (27.3)	0.354
≥4	112 (71.3)	149 (43.4)		34 (64.2)	72 (72.7)	
TI-RADS, n			<0.001			<0.001
3	102	13		35	3	
4–5	55	330		18	96	

P value: two-tailed test, <0.05 were considered statistically significant. PTC, papillary thyroid carcinoma; IQR, interquartile range; TSH, thyrotropin; SII, systemic immune-inflammation index; LMR, lymphocyte-to-monocyte ratio; TI-RADS, Thyroid Imaging Reporting and Data System.

Table 2 Multivariate logistic regression analysis of potential predictors of PTC in the primary cohort

Risk Factors	β	Odds ratio (95% CI)	P
Age (years)	–0.070	0.932 (0.901–0.963)	<0.001
Echogenicity	1.511	4.533 (1.711–12.542)	0.003
Margin	1.664	5.281 (2.540–11.197)	<0.001
Calcification	1.003	2.429 (1.286–5.928)	0.010
Composition	0.939	2.557 (0.880–7.520)	0.084
Tall than wide	2.964	19.371 (9.239–44.056)	<0.001
TSH (mIU/mL)	0.305	1.357 (0.673–2.744)	0.393
SII	0.558	1.748 (0.845–3.662)	0.134
LMR	–1.271	0.280 (0.131–0.579)	<0.001

PTC, papillary thyroid carcinoma; TSH, thyrotropin; SII, systemic immune-inflammation index; LMR, lymphocyte-to-monocyte ratio.

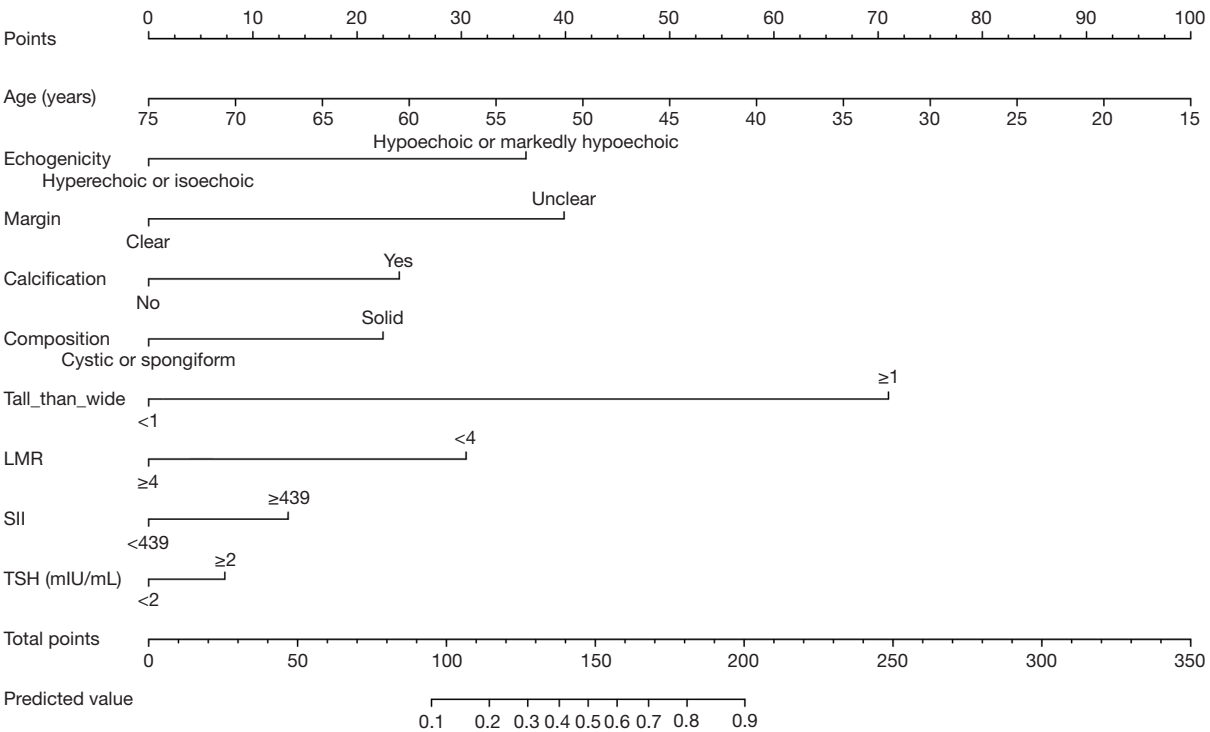

Figure 2 Developed nomogram. The nomogram was developed in the primary cohort. LMR, lymphocyte-to-monocyte ratio; TSH, thyrotropin; SII, systemic immune-inflammation index.

and LMR (OR: 0.280, 95% CI: 0.131–0.579) demonstrated statistical significance. Composition (OR: 2.557, 95% CI: 0.800–7.520), TSH (OR:1.357, 95% CI: 0.673–2.744), and SII (OR: 1.748, 95% CI: 0.845–3.662) were not statistically significant. The multivariate analysis coefficients were used to develop the following prediction equation for PTC: Y = –0.070 × (age) + 1.511 × (echogenicity) + 1.664 × (margin) + 1.003 × (calcification) + 0.939 × (composition) + 2.964 × (tall than wide) + 0.305 × (TSH) + 0.558 × (SII) – 1.271 × (LMR) + 0.327, where the unit of the TSH was mIU/L, the SII and LMR was 10^9/L, echogenicity was scored as 1 for hypoechoic or markedly hypoechoic and 0 for hyperechoic

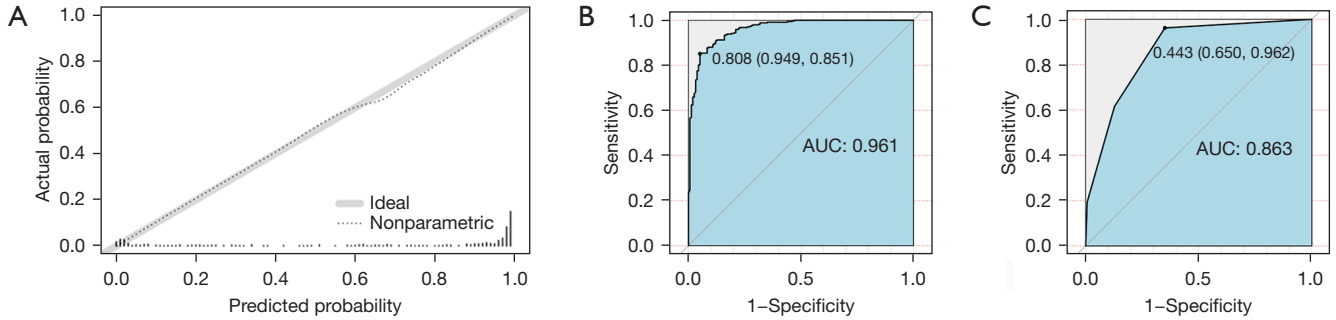

Figure 3 Calibration curve (A) and ROC curve (B) of nomogram and ROC curve (C) of Thyroid Imaging Reporting and Data System classification in the primary cohort. The solid dot indicates sensitivity and specificity with the maximal value of Youden's index. ROC, receiver operating characteristic; AUC, area under the curve.

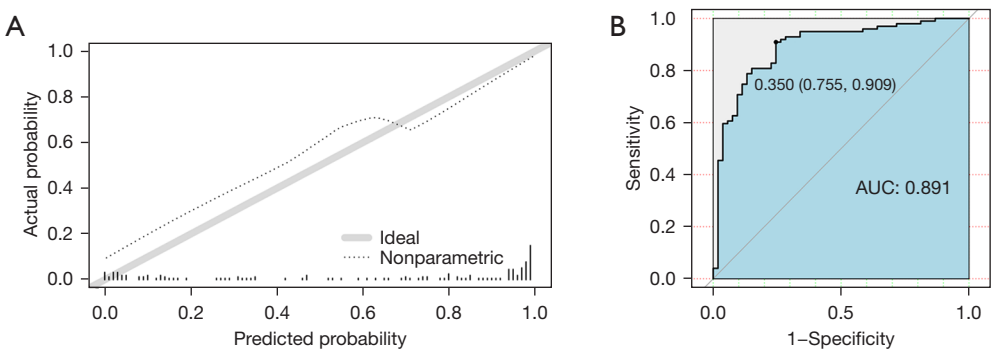

Figure 4 Calibration curve (A) and ROC curve (B) of nomogram in the validation cohort. ROC, receiver operating characteristic; AUC, area under the curve.

or isoechoic, margin was scored as 1 for unclear and 0 for clear, calcification was scored as 1 for calcification and 0 for no calcification, composition was scored as 1 for solid and 0 for cystic or spongiform, and tall than wide was scored as 1 for taller than wide and 0 for wider than tall.

Performance of the nomogram in the primary cohort

Prediction and observation of PTC probabilities showed good agreement in the calibration curves of the nomogram (*Figure 3A*). The brier score of 0.069 indicated that there was no departure from the ideal fit. From the ROC curve, it was determined that the regression equation's prediction probability was appropriate (*Figure 3B*), and its diagnostic efficacy is superior to the TI-RADA classification (*Figure 3C*). This model's accuracy was demonstrated by the AUC, which was 0.961 (95% CI: 0.945–0.978). In contrast, the AUC for TI-RADS classification was 0.863 (95% CI: 0.828–0.898). Youden's index was used to filter the ROC curve to the ideal boundary value of 0.800. When Y was greater than 0.808, the model correctly anticipated PTC. In the PTC group, 308 of the 343 cases and 146 of the 157 cases in the non-PTC group had accurate predictions. This model's accuracy, sensitivity, and specificity of the predictions were, in order, 88.2%, 85.1%, and 94.9%, respectively.

Validation of the nomogram

Internal validation

The prediction model produced a C-index of 0.961 and a brier score of 0.068 using the enhanced bootstrap method for internal validation of the diagnostic model.

External validation

The probability of PTC in the validation cohort showed good calibration (*Figure 4A*). the brier score was 0.125. the AUC of the nomogram for the prediction of PTC was 0.891 (95% CI: 0.835–0.947) (*Figure 4B*). In the external

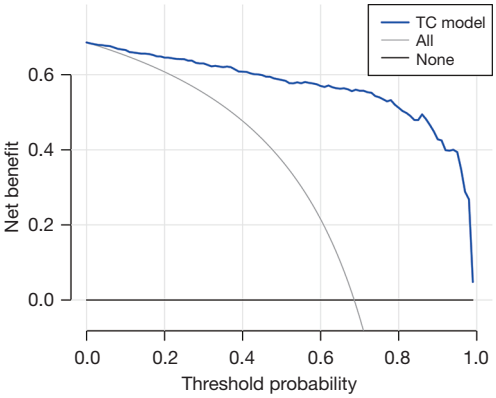

Figure 5 Decision curve analysis for the nomogram. The y-axis measures the net benefit. The blue line represents the nomogram. The grey line represents the assumption that all patients are diagnosed with papillary thyroid carcinoma. The black line represents the assumption that no patients are diagnosed with PTC. TC, thyroid carcinoma; PTC, papillary thyroid carcinoma.

validation, 44 of the 53 non-PTC instances and 83 of the 99 PTC cases were properly predicted. In this dataset, the model's accuracy, sensitivity, and specificity of the prediction were 85.5%, 90.9%, and 75.5%, respectively.

Clinical use

Figure 5 shows the decision curve analysis for the nomogram. The decision curve demonstrated that the nomogram is more advantageous for predicting PTC than either the treat-all-patients scheme or the treat-none scheme.

Discussion

In this work, we used the TSH, inflammatory markers, and findings on thyroid nodule ultrasonography to construct a simple prediction model for the preoperative evaluation of PTC. The diagnostic efficacy of this model is better than that of TI-RADS classification. In external validation, excellent results were obtained for the discrimination, calibration, accuracy, sensitivity and specificity of the prediction model, which indicated that the model could be applied to patients with thyroid nodules outside of both datasets. The probability of a patient being diagnosed with PTC can be obtained by calculating the score of the corresponding index on the nomogram. For the preoperative evaluation of PTC, this is the first prediction model based on ultrasound and inflammatory markers.

TSH is a dimeric glycoprotein secreted by the pituitary gland which is essential for the regulation of blood supply to the thyroid gland, cellular value-added, and the synthesis and secretion of thyroxine. In the treatment of thyroid cancer, TSH is crucial. In our investigation, the PTC group's serum TSH was statistically different from the non-PTC group's, with differences being statistically significant for both univariate and multivariate logistic regression analysis. As a potential causal mechanism for the development of thyroid tumors, certain investigations have suggested a positive correlation between blood TSH and PTC (17). Additionally, high-risk individuals are treated for thyroid cancer with TSH suppression, and there is evidence that this lowers mortality (18). The results of a study showed that 81.3% of patients had TSH levels between 0.5 and 4.5 mIU/L. Among them, 10.8% had TSH levels between 3 and 4.5 mIU/L, and which risk of malignancy was 38.2%. 7.9% had TSH levels less than or equal to 0.4 mIU/L, and which risk of malignancy was 16%. The results of this study also indicate that the mean preoperative TSH levels in patients with malignant tumors are significantly higher than those in patients with benign tumors and that TSH is an accurate indicator of cancer when TSH levels exceed 4.5 mIU/L (19). Through the activation of the PI3K-AKT and RAS-BRAF pathways, serum TSH may contribute to the growth of thyroid cancer (20,21). Currently, many scholars have found that TSH levels are intimately linked to thyroid cancer, and high levels of TSH can be considered an independent predictor of thyroid cancer, which is consistent with the results of our study (22).

A growing body of clinical evidence suggests that tumor-associated immune cells play a vital role in the development of cancer and that circulating immune cells are involved in the long-term prognosis of a wide range of cancers (11,23). An essential component of innate immunity, neutrophils are a subtype of leukocytes that can remove pathogens through recruitment (24). It is involved in several intricate physiological and pathological processes, including cancer development, in addition to acute inflammation caused by conditions like infection (25). There is mounting evidence that neutrophils contribute to the development, spread, and growth of tumors. Elevated neutrophils inhibit the secretion of TNF-A, leading to increased VEGF release, and overexpression of VEGF promotes tumor neovascularization, thereby accelerating tumor growth and metastasis (26,27). TGF-beta, VEGF, and platelet-derived growth factors, which play a growing role in tumor

progression and metastasis, can be secreted by platelets (28). Additionally, there is evidence to suggest that platelets facilitate tumor spread by enhancing neovascularization, impairing defensive mechanisms, and priming the milieu for metastasis (29). The number and percentage of lymphocytes can reflect the immune dynamics. When the number of lymphocytes is relatively low, it may indicate that fewer lymphocytes are present in the paracancerous tissues, which lowers their ability to mediate an immune response against the tumor, creating a tumor microenvironment favorable for the growth and metastasis of cancer cells and resulting in a poor prognosis for the patient (30-32). Tumor-associated macrophages (TAMs) derived from circulating mononuclear cells play a crucial role in promoting tumor progression and metastasis (33). Epidermal growth factor (EGF), vascular endothelial growth factor (VEGF), IL-6, IL-10, and matrix metalloproteinases are secreted by TAMs, which promote tumor tissue angiogenesis, modification of the extracellular matrix, and invasion and metastasis of tumor cells (34,35). Low LMR is now known to be an independent risk factor for recurrence in patients with curatively resected PTC, according to a recent study by Yokota *et al.* (36). High SII is a reliable biomarker for predicting central lymph node metastases in PTC, according to Zhang *et al.*, this report backs up the findings of this investigation (37).

In the present study, low age, hypoechoic or markedly hypoechoic, unclear margin, calcification, and taller-than-wide were considered independent predictors of thyroid cancer. One of the significant variables that have been strongly linked to the diagnosis of TCs is age. Sharen *et al.* concluded that (38), compared to young and middle-aged groups, the detection rate of TCs was lower in the population over 60. PTC manifests on conventional ultrasonography as opaque hypoechoic nodules, which are frequently associated with microcalcification and tall-than-wide ≥1 (39). There is an association between calcification and thyroid cancer. Microcalcifications are generally considered to be a reliable indicator of malignancy (40). Cai *et al.* suggested that a dismal prognosis was suggested by the pathology's discovery of psammoma bodies (41) and pathological psammoma bodies appear on ultrasound as microcalcifications (42). Echogenicity refers to the solid component of the nodule relative to the echogenic level of the thyroid parenchyma and the cervical zonules. Most malignant thyroid tumors were hypoechoic (62.5–87.2%) and the risk of malignancy was higher in hypoechoic nodules (20.6–70.4%) than in isoechoic (8.6–13.4%) or hyperechoic (0–18.2%) nodules (43). Our findings support previous work (44) that taller-than-wide is a specific way to distinguish between benign and malignant thyroid nodules. This finding shows that benign nodules develop parallel to the normal tissue plane while malignant nodules develop across it. Due to the invasive nature of malignant tumors, the margin with the surrounding normal tissues is indistinguishable, and the presentation in ultrasound is unclear margins. Chng *et al.* reported that significantly greater percentages of malignancy were present in nodules with unclear margins than in benign nodules (45).

The gold standard for identifying benign from malignant thyroid nodules is pathological evidence. A fine needle aspiration biopsy is an invasive test that can result in more invasiveness and more problems, such as bleeding. The ideal approach for thyroid screening is ultrasonography since it is non-invasive (46). PTC is diagnosed clinically with conventional ultrasound, which has a diagnostic accuracy of 74–82% (47). However, combining suspicious ultrasound features, TSH, and inflammatory markers can provide better diagnostic accuracy than the TI-RADS classification. In our study, the accuracy, sensitivity, and specificity of the prediction of this model were 88.2%, 85.1%, and 94.9%, respectively, and in the external validation, the above indicators were 85.5%, 90.9% and 75.5% respectively. Meanwhile, preoperative ultrasound features, TSH and inflammatory markers are some of the simple tests which are economical and convenient. This is the main advantage of this study's results.

The study's main drawback is that it is based on a study that was carried out in one institution retrospectively. Also, the sample size included is small and most of the analyses are qualitative and subjective indicators. Second, the data for the external validation of this study were obtained from the same institution and different periods, which means might introduce bias. Accordingly, further external validation based on Spatio-temporal is necessary. Finally, the model we have constructed does not involve other types of thyroid cancer. Therefore, in subsequent studies, it is essential to construct diagnostic models to discriminate other types of thyroid cancer from benign thyroid nodules.

Conclusions

In summary, utilizing preoperative ultrasound characteristics, TSH, and inflammatory markers, we created and validated a straightforward and accurate preoperative prediction model and nomogram for PTC in this investigation, which may provide an additional tool for diagnostic prediction that can

be used to accurately advise physicians and patients, allowing for targeted treatment of PTC. With the help of this model, preoperative PTC diagnosis may be made more accurately.

Acknowledgments

Funding: None.

Footnote

Reporting Checklist: The authors have completed the TRIPOD reporting checklist. Available at https://tcr.amegroups.com/article/view/10.21037/tcr-22-2478/rc

Data Sharing Statement: Available at https://tcr.amegroups.com/article/view/10.21037/tcr-22-2478/dss

Peer Review File: Available at https://tcr.amegroups.com/article/view/10.21037/tcr-22-2478/prf

Conflicts of Interest: All authors have completed the ICMJE uniform disclosure form (available at https://tcr.amegroups.com/article/view/10.21037/tcr-22-2478/coif). The authors have no conflicts of interest to declare.

Ethical Statement: The authors are accountable for all aspects of the work in ensuring that questions related to the accuracy or integrity of any part of the work are appropriately investigated and resolved. The study was conducted in accordance with the Declaration of Helsinki (as revised in 2013). The study was approved by the Ethics Committee of The First Affiliated Hospital of Xinjiang Medical University (No. K202206-02) and individual consent for this retrospective analysis was waived.

References

1. Wu Q, Qu Y, Li Y, et al. Logistic regression analysis of contrast-enhanced ultrasound and conventional ultrasound of follicular thyroid carcinoma and follicular adenoma. Gland Surg 2021;10:2890-900.
2. Lim H, Devesa SS, Sosa JA, et al. Trends in Thyroid Cancer Incidence and Mortality in the United States, 1974-2013. JAMA 2017;317:1338-48.
3. Pellegriti G, Frasca F, Regalbuto C, et al. Worldwide increasing incidence of thyroid cancer: update on epidemiology and risk factors. J Cancer Epidemiol 2013;2013:965212.
4. Vaccarella S, Franceschi S, Bray F, et al. Worldwide Thyroid-Cancer Epidemic? The Increasing Impact of Overdiagnosis. N Engl J Med 2016;375:614-7.
5. Siegel RL, Miller KD, Jemal A. Cancer statistics, 2019. CA Cancer J Clin 2019;69:7-34.
6. Lubitz CC, Kong CY, McMahon PM, et al. Annual financial impact of well-differentiated thyroid cancer care in the United States. Cancer 2014;120:1345-52.
7. Morris LG, Myssiorek D. Improved detection does not fully explain the rising incidence of well-differentiated thyroid cancer: a population-based analysis. Am J Surg 2010;200:454-61.
8. Brito JP, Gionfriddo MR, Al Nofal A, et al. The accuracy of thyroid nodule ultrasound to predict thyroid cancer: systematic review and meta-analysis. J Clin Endocrinol Metab 2014;99:1253-63.
9. Kwak JY, Jung I, Baek JH, et al. Image reporting and characterization system for ultrasound features of thyroid nodules: multicentric Korean retrospective study. Korean J Radiol 2013;14:110-7.
10. Pagano L, Mele C, Sama MT, et al. Thyroid cancer phenotypes in relation to inflammation and autoimmunity. Front Biosci (Landmark Ed) 2018;23:2267-82.
11. Singh R, Mishra MK, Aggarwal H. Inflammation, Immunity, and Cancer. Mediators Inflamm 2017;2017:6027305.
12. Chan JC, Chan DL, Diakos CI, et al. The Lymphocyte-to-Monocyte Ratio is a Superior Predictor of Overall Survival in Comparison to Established Biomarkers of Resectable Colorectal Cancer. Ann Surg 2017;265:539-46.
13. Chen JH, Zhai ET, Yuan YJ, et al. Systemic immune-inflammation index for predicting prognosis of colorectal cancer. World J Gastroenterol 2017;23:6261-72.
14. Grani G, Ramundo V, Verrienti A, et al. Thyroid hormone therapy in differentiated thyroid cancer. Endocrine 2019;66:43-50.
15. Kim D, Park JW. Clinical implications of preoperative thyrotropin serum concentrations in patients who

underwent thyroidectomy for nonfunctioning nodule(s). J Korean Surg Soc 2013;85:15-9.
16. Tessler FN, Middleton WD, Grant EG, et al. ACR Thyroid Imaging, Reporting and Data System (TI-RADS): White Paper of the ACR TI-RADS Committee. J Am Coll Radiol 2017;14:587-95.
17. McLeod DS, Watters KF, Carpenter AD, et al. Thyrotropin and thyroid cancer diagnosis: a systematic review and dose-response meta-analysis. J Clin Endocrinol Metab 2012;97:2682-92.
18. Biondi B, Cooper DS. Thyroid Hormone Suppression Therapy. Endocrinol Metab Clin North Am 2019;48:227-37.
19. Al Dawish MA, Alwin Robert A, Thabet MA, et al. Thyroid Nodule Management: Thyroid-Stimulating Hormone, Ultrasound, and Cytological Classification System for Predicting Malignancy. Cancer Inform 2018;17:1176935118765132.
20. Kouniavsky G, Zeiger MA. Thyroid tumorigenesis and molecular markers in thyroid cancer. Curr Opin Oncol 2010;22:23-9.
21. Brzezianska E, Pastuszak-Lewandoska D. A minireview: the role of MAPK/ERK and PI3K/Akt pathways in thyroid follicular cell-derived neoplasm. Front Biosci (Landmark Ed) 2011;16:422-39.
22. Kim HK, Yoon JH, Kim SJ, et al. Higher TSH level is a risk factor for differentiated thyroid cancer. Clin Endocrinol (Oxf) 2013;78:472-7.
23. Greten FR, Grivennikov SI. Inflammation and Cancer: Triggers, Mechanisms, and Consequences. Immunity 2019;51:27-41.
24. Kolaczkowska E, Kubes P. Neutrophil recruitment and function in health and inflammation. Nat Rev Immunol 2013;13:159-75.
25. Jaillon S, Galdiero MR, Del Prete D, et al. Neutrophils in innate and adaptive immunity. Semin Immunopathol 2013;35:377-94.
26. Dumitru CA, Lang S, Brandau S. Modulation of neutrophil granulocytes in the tumor microenvironment: mechanisms and consequences for tumor progression. Semin Cancer Biol 2013;23:141-8.
27. Gong W, Yang S, Yang X, et al. Blood preoperative neutrophil-to-lymphocyte ratio is correlated with TNM stage in patients with papillary thyroid cancer. Clinics (Sao Paulo) 2016;71:311-4.
28. Stone RL, Nick AM, McNeish IA, et al. Paraneoplastic thrombocytosis in ovarian cancer. N Engl J Med 2012;366:610-8.
29. Gkolfinopoulos S, Jones RL, Constantinidou A. The Emerging Role of Platelets in the Formation of the Micrometastatic Niche: Current Evidence and Future Perspectives. Front Oncol 2020;10:374.
30. Stotz M, Pichler M, Absenger G, et al. The preoperative lymphocyte to monocyte ratio predicts clinical outcome in patients with stage III colon cancer. Br J Cancer 2014;110:435-40.
31. Chen L, Zhang F, Sheng XG, et al. Decreased pretreatment lymphocyte/monocyte ratio is associated with poor prognosis in stage Ib1-IIa cervical cancer patients who undergo radical surgery. Onco Targets Ther 2015;8:1355-62.
32. Sylman JL, Mitrugno A, Atallah M, et al. The Predictive Value of Inflammation-Related Peripheral Blood Measurements in Cancer Staging and Prognosis. Front Oncol 2018;8:78.
33. Katoh H, Watanabe M. Myeloid-Derived Suppressor Cells and Therapeutic Strategies in Cancer. Mediators Inflamm 2015;2015:159269.
34. Hanahan D, Weinberg RA. Hallmarks of cancer: the next generation. Cell 2011;144:646-74.
35. Chanmee T, Ontong P, Konno K, et al. Tumor-associated macrophages as major players in the tumor microenvironment. Cancers (Basel) 2014;6:1670-90.
36. Yokota M, Katoh H, Nishimiya H, et al. Lymphocyte-Monocyte Ratio Significantly Predicts Recurrence in Papillary Thyroid Cancer. J Surg Res 2020;246:535-43.
37. Zhang Z, Xia F, Wang W, et al. The systemic immune-inflammation index-based model is an effective biomarker on predicting central lymph node metastasis in clinically nodal-negative papillary thyroid carcinoma. Gland Surg 2021;10:1368-73.
38. Sharen G, Zhang B, Zhao R, et al. Retrospective epidemiological study of thyroid nodules by ultrasound in asymptomatic subjects. Chin Med J (Engl) 2014;127:1661-5.
39. Liu Y, He L, Yin G, et al. Association analysis and the clinical significance of BRAF gene mutations and ultrasound features in papillary thyroid carcinoma. Oncol Lett 2019;18:2995-3002.
40. Ferreira LB, Gimba E, Vinagre J, et al. Molecular Aspects of Thyroid Calcification. Int J Mol Sci 2020;21:7718.
41. Cai YF, Wang QX, Ni CJ, et al. The Clinical Relevance of Psammoma Body and Hashimoto Thyroiditis in Papillary Thyroid Carcinoma: A Large Case-control Study. Medicine (Baltimore) 2015;94:e1881.
42. Jia ZY, Wu XL, Zhang YH, et al. The correlation between

ultrasonographic features, bFGF, and the local invasiveness of thyroid papillary carcinoma. Medicine (Baltimore) 2020;99:e20644.
43. Shin JH, Baek JH, Chung J, et al. Ultrasonography Diagnosis and Imaging-Based Management of Thyroid Nodules: Revised Korean Society of Thyroid Radiology Consensus Statement and Recommendations. Korean J Radiol 2016;17:370-95.
44. Pang T, Huang L, Deng Y, et al. Logistic regression analysis of conventional ultrasonography, strain elastosonography, and contrast-enhanced ultrasound characteristics for the differentiation of benign and malignant thyroid nodules. PLoS One 2017;12:e0188987.
45. Chng CL, Kurzawinski TR, Beale T. Value of sonographic features in predicting malignancy in thyroid nodules diagnosed as follicular neoplasm on cytology. Clin Endocrinol (Oxf) 2015;83:711-6.
46. Haugen BR, Alexander EK, Bible KC, et al. 2015 American Thyroid Association Management Guidelines for Adult Patients with Thyroid Nodules and Differentiated Thyroid Cancer: The American Thyroid Association Guidelines Task Force on Thyroid Nodules and Differentiated Thyroid Cancer. Thyroid 2016;26:1-133.
47. Zhang B, Jiang YX, Liu JB, et al. Utility of contrast-enhanced ultrasound for evaluation of thyroid nodules. Thyroid 2010;20:51-7.

Cite this article as: Tang ZW, Li XX, Luo J. Development and validation of the nomogram based on ultrasound, thyroid stimulating hormone, and inflammatory marker in papillary thyroid carcinoma: a case-control study. Transl Cancer Res 2023;12(3):490-501. doi: 10.21037/tcr-22-2478

